

One-Loop Amplitudes for $e^+e^- \rightarrow \bar{q}q\bar{Q}Q$

Zvi Bern[#]

*Department of Physics and Astronomy
 University of California, Los Angeles
 Los Angeles, CA 90095
 bern@physics.ucla.edu*

Lance Dixon^{*}

*Stanford Linear Accelerator Center
 Stanford University
 Stanford, CA 94309
 lance@slac.stanford.edu*

David A. Kosower and Stefan Weinzierl

*Service de Physique Théorique[†]
 Centre d'Etudes de Saclay
 F-91191 Gif-sur-Yvette cedex, France
 kosower@spht.saclay.cea.fr
 stefanw@spht.saclay.cea.fr*

Abstract

We present the one-loop helicity amplitudes for processes involving a vector boson V ($V = W, Z$, or γ^*) and four massless quarks, $0 \rightarrow V\bar{q}q\bar{Q}Q$, where V couples to a massless lepton pair. These amplitudes are required for next-to-leading order $\mathcal{O}(\alpha_s^3)$ numerical programs for four-jet production at e^+e^- colliders, for W, Z or Drell-Yan production in association with two jets at hadron colliders, and for three-jet production in deeply inelastic scattering experiments. We obtained the amplitudes presented here by using their analytic properties to constrain their form.

Submitted to Nuclear Physics B

[#]Research supported in part by the US Department of Energy under grant DE-FG03-91ER40662 and in part by the Alfred P. Sloan Foundation under grant BR-3222.

^{*}Research supported by the US Department of Energy under grant DE-AC03-76SF00515.

[†]Laboratory of the *Direction des Sciences de la Matière* of the *Commissariat à l'Energie Atomique* of France.

1. Introduction

Electron-positron annihilation provides a clean experimental laboratory for studying jet properties. Leading-order predictions for the production of up to five jets have been available for quite some time [1,2,3,4], but the reduction of theoretical uncertainties requires next-to-leading-order (NLO) QCD corrections. The NLO matrix elements for three-jet production and other $\mathcal{O}(\alpha_s)$ observables are also known [3], and numerical programs implementing these corrections [5] have been widely used to extract a precise value of α_s from hadronic event shapes at the Z pole [6].

Next-to-leading order corrections for more complicated processes are required, however, if we wish to use QCD in probing for new physics in other standard model processes. In e^+e^- annihilation, for example, four-jet production is the lowest-order process in which the quark and gluon color charges can be measured independently. Four-jet production is thus sensitive to the presence of light colored fermions such as gluinos [7]. At LEP 2 the process $e^+e^- \rightarrow (\gamma^*, Z) \rightarrow 4 \text{ jets}$ is a background to threshold production of W pairs, when both W s decay hadronically. The one-loop matrix elements required for an NLO study of four-jet production are also needed for a next-to-next-to-leading (NNLO) study of three-jet production at the Z pole. Such a study (which awaits the computation of certain two-loop matrix elements as well) would be desirable in order to reduce the theoretical uncertainties in determining α_s via this process.

In this paper we present analytic formulas for the one-loop helicity amplitudes for electron-positron annihilation into four-quarks, $e^+e^- \rightarrow (\gamma^*, Z) \rightarrow \bar{q}q\bar{Q}Q$. Together with the leading-in-color matrix elements for production of two quarks and two gluons, $e^+e^- \rightarrow \bar{q}qgg$ [8,9], the leading-color parts of these amplitudes have already been incorporated into an NLO program for $e^+e^- \rightarrow 4 \text{ jets}$ [10]. The same amplitudes presented here may also be used in computations of W or $Z + 2 \text{ jet}$ production at hadron colliders and three-jet production in deeply inelastic scattering. Glover and Miller [11] have also recently reported on a calculation of the squared one-loop matrix elements for $e^+e^- \rightarrow \gamma^* \rightarrow \bar{q}q\bar{Q}Q$, summed over helicities and expressed in terms of Lorentz scalar products of the quark four-momenta, rather than the spinor products that we employ. A comparison of their results with those presented in this paper will be useful.

Recent years have seen a number of technical advances in the computation of one-loop amplitudes, which the authors have surveyed in a recent review article [12]. These advances have made possible the calculation of all one-loop five-parton processes [13,14,15], as well as of a number of infinite sequences of one-loop amplitudes [16,17,18,19]. The general strategy employed in this paper (and in a subsequent paper on $e^+e^- \rightarrow \bar{q}qgg$ [8,9]) is to obtain amplitudes from their analytic structure. In particular, we use the constraints of unitarity [20,18,19,21] and factorization [16,22], as summarized in ref. [12]. This approach leads to relatively compact expressions, as compared

with those obtained from a traditional, diagrammatic computation. In this approach, amplitudes obtained previously are recycled to obtain new amplitudes; manifest gauge invariance is therefore maintained. In a Feynman diagram approach each diagram alone is not gauge invariant, and are often individually much more complicated than a final sum over diagrams.

We use helicity methods [23,24] since they lead to relatively compact expressions for the amplitudes, and retain all spin information. We also make use of color decompositions [25] to help simplify the analytic structures that must be computed. As a check, we have verified numerically that the amplitudes presented in this paper agree with a direct Feynman diagram calculation we performed.

The paper is organized as follows. In section 2, we briefly describe helicity methods and color decompositions. We give the amplitudes, together with a brief description of the calculational methods, in section 3; we describe the contribution proportional to the axial vector coupling of the Z to the t, b quark isodoublet in subsection 3.4. A summary is included in section 4. We collect descriptions of various integral functions appearing in the amplitudes in an appendix.

2. Basic Tools

In this section, we briefly review two of the basic tools useful for expressing amplitudes in a compact form: the spinor helicity method and color decompositions. The reader is referred to review articles [26] and references therein for further details.

2.1 Spinor Helicity

In explicit calculations it is usually convenient to use a helicity basis, where all quantities are rewritten in terms of Weyl spinors $|k^\pm\rangle$. Although there are no external gluons in the final $e^+e^- \rightarrow \bar{q}q\bar{Q}Q$ helicity amplitudes, they appear as intermediate states in various unitarity cuts and factorization limits that are used to construct the amplitudes. We made use of the gluon polarization vectors of Xu, Zhang and Chang [23,24],

$$\varepsilon_\mu^+(k; q) = \frac{\langle q^- | \gamma_\mu | k^- \rangle}{\sqrt{2} \langle q k \rangle}, \quad \varepsilon_\mu^-(k; q) = \frac{\langle q^+ | \gamma_\mu | k^+ \rangle}{\sqrt{2} [k q]}, \quad (2.1)$$

where k is the gluon momentum and q is an arbitrary null ‘reference momentum’ which drops out of final gauge-invariant amplitudes. The plus and minus labels on the polarization vectors refer to the gluon helicities. Our (crossing-symmetric) convention takes all particles to be outgoing, and labels the helicity and particle vs. antiparticle assignment accordingly. (That is, we write the amplitudes for the process $0 \rightarrow V\bar{q}q\bar{Q}Q$.) For incoming (negative energy) momenta the helicity and particle

vs. antiparticle assignment are reversed. It is convenient to define

$$\begin{aligned}
\langle i j \rangle &\equiv \langle k_i^- | k_j^+ \rangle, & [i j] &\equiv \langle k_i^+ | k_j^- \rangle, \\
\langle i | l | j \rangle &\equiv \langle k_i^- | \not{k}_l | k_j^- \rangle, & \langle i | (l + m) | j \rangle &\equiv \langle k_i^- | (\not{k}_l + \not{k}_m) | k_j^- \rangle, \\
\langle i^- | (l + m)(n + r) \cdots | j^+ \rangle &\equiv \langle k_i^- | (\not{k}_l + \not{k}_m)(\not{k}_n + \not{k}_r) \cdots | k_j^+ \rangle,
\end{aligned} \tag{2.2}$$

for the spinor products, which is the notation we shall use to quote the results. Here all the momenta k_i are massless. The spinor inner products $\langle i j \rangle$, $[i j]$ are antisymmetric and satisfy $\langle i j \rangle [j i] = 2k_i \cdot k_j \equiv s_{ij}$.

To maximize the benefit obtained from the spinor helicity formalism for loop amplitudes we must choose a compatible regularization scheme. In conventional dimensional regularization [27], the polarization vectors are $(4 - 2\epsilon)$ -dimensional, which is incompatible with the spinor helicity method's use of four-dimensional polarizations. To avoid this problem, we modify the regularization scheme so all helicity states are four-dimensional and only the loop momentum is continued to $(4 - 2\epsilon)$ dimensions. This is the four-dimensional-helicity (FDH) scheme [28], which has been shown to be equivalent at one-loop [29] to an appropriate helicity formulation of Siegel's dimensional-reduction scheme ($\overline{\text{DR}}$) [30]. The conversion between schemes has been given in ref. [29]; there is no loss of generality in choosing the FDH/ $\overline{\text{DR}}$ scheme.

2.2 Color Decomposition

In this section we describe a color decomposition [25] of the one-loop amplitude for $e^+e^- \rightarrow \bar{q}q\bar{Q}Q$, in terms of group-theoretic factors (color structures) multiplied by kinematic functions called *partial amplitudes*. Because of the crossing symmetry of the spinor products [24] and of the integral functions (discussed in the appendix), these partial amplitudes may also be used to obtain the one-loop contributions to Z or $W + 2$ jet production at hadron colliders or three jet production in deeply inelastic scattering. (For the case of the W , only the coupling constants need be changed in the formulæ given below.)

The partial amplitudes are defined to be the coefficients of the various color structures. Consider the amplitude $\mathcal{A}_6(1_q, 2_{\bar{Q}}, 3_Q, 4_{\bar{q}}; 5_{\bar{e}}, 6_e)$. At tree-level its decomposition is

$$\begin{aligned}
\mathcal{A}_6^{\text{tree}}(1_q, 2_{\bar{Q}}, 3_Q, 4_{\bar{q}}) &= 2e^2 g^2 \left[\left(-Q^q + v_{L,R}^e v_{L,R}^q \mathcal{P}_Z(s_{56}) \right) A_6^{\text{tree}}(1_q, 2_{\bar{Q}}, 3_Q, 4_{\bar{q}}) \right. \\
&\quad \left. + \left(-Q^Q + v_{L,R}^e v_{L,R}^Q \mathcal{P}_Z(s_{56}) \right) A_6^{\text{tree}}(3_Q, 4_{\bar{q}}, 1_q, 2_{\bar{Q}}) \right] \\
&\quad \times \left(\delta_{i_1}^{\bar{i}_2} \delta_{i_3}^{\bar{i}_4} - \frac{1}{N_c} \delta_{i_1}^{\bar{i}_4} \delta_{i_3}^{\bar{i}_2} \right),
\end{aligned} \tag{2.3}$$

where we have suppressed the 5, 6 labels of the electron pair, e is the QED coupling, g the QCD coupling, Q^q (Q^Q) is the charge of quark q (quark Q) in units of e , and the left- and right-handed

couplings are

$$\begin{aligned} v_L^e &= \frac{-1 + 2 \sin^2 \theta_W}{\sin 2\theta_W}, & v_R^e &= \frac{2 \sin^2 \theta_W}{\sin 2\theta_W}, \\ v_L^q &= \frac{\pm 1 - 2Q^q \sin^2 \theta_W}{\sin 2\theta_W}, & v_R^q &= -\frac{2Q^q \sin^2 \theta_W}{\sin 2\theta_W}, \end{aligned} \quad (2.4)$$

where θ_W is the Weinberg angle. Eq. (2.3) contains the ratio of the Z and photon propagators,

$$\mathcal{P}_Z(s) = \frac{s}{s - M_Z^2 + i\Gamma_Z M_Z} \quad (2.5)$$

where M_Z and Γ_Z are the mass and width of the Z . We have given the decomposition for a general $SU(N_c)$ gauge group; $N_c = 3$ for QCD. The two signs in v_L^q correspond to up (+) and down (-) type quarks.

The subscripts L and R refer to whether the particle to which the Z couples is left- or right-handed. That is, v_R^q is to be used for the configuration where the quark (leg 1) has plus helicity and the anti-quark (leg 4) has minus helicity, which we denote by the shorthand $(1_q^+, 4_{\bar{q}}^-)$. Similarly, v_L^q corresponds to the configuration $(1_q^-, 4_{\bar{q}}^+)$. Because the electron and positron are incoming in e^+e^- annihilation, our outgoing-momenta notation reverses their helicities and particle vs. anti-particle assignment. Thus, v_R^e corresponds to the helicity configuration $(5_{\bar{e}}^-, 6_e^+)$ whereas v_L^e corresponds to the configuration $(5_{\bar{e}}^+, 6_e^-)$.

We have defined the tree and one-loop partial amplitudes A_6^{tree} and $A_{6;i}$ to include a photon propagator. The ratio $\mathcal{P}_Z(s_{56})$ appearing in eq. (2.3) then replaces the photon propagator with a Z propagator. This form of the amplitude is convenient for checking that amplitudes properly reduce to lower-point amplitudes when the e^+ and e^- momenta are taken to be collinear.

At one loop there are three partial amplitudes,

$$\begin{aligned} \mathcal{A}_6^{1\text{-loop}}(1_q, 2_{\bar{Q}}, 3_Q, 4_{\bar{q}}) = & \\ & 2e^2 g^4 \left[\left(-Q^q + v_{L,R}^e v_{L,R}^q \mathcal{P}_Z(s_{56}) \right) \left[N_c \delta_{i_1}^{\bar{i}_2} \delta_{i_3}^{\bar{i}_4} A_{6;1}(1_q, 2_{\bar{Q}}, 3_Q, 4_{\bar{q}}) + \delta_{i_1}^{\bar{i}_4} \delta_{i_3}^{\bar{i}_2} A_{6;2}(1_q, 2_{\bar{Q}}, 3_Q, 4_{\bar{q}}) \right] \right. \\ & + \left(-Q^Q + v_{L,R}^e v_{L,R}^Q \mathcal{P}_Z(s_{56}) \right) \left[N_c \delta_{i_1}^{\bar{i}_2} \delta_{i_3}^{\bar{i}_4} A_{6;1}(3_Q, 4_{\bar{q}}, 1_q, 2_{\bar{Q}}) + \delta_{i_1}^{\bar{i}_4} \delta_{i_3}^{\bar{i}_2} A_{6;2}(3_Q, 4_{\bar{q}}, 1_q, 2_{\bar{Q}}) \right] \\ & \left. + \frac{v_{L,R}^e}{\sin 2\theta_W} \mathcal{P}_Z(s_{56}) \left(\delta_{i_1}^{\bar{i}_2} \delta_{i_3}^{\bar{i}_4} - \frac{1}{N_c} \delta_{i_1}^{\bar{i}_4} \delta_{i_3}^{\bar{i}_2} \right) A_{6;3}(1_q, 2_{\bar{Q}}, 3_Q, 4_{\bar{q}}) \right]. \end{aligned} \quad (2.6)$$

Note the additional factor of N_c in the color-tensor coefficients of $A_{6;1,2}$ compared to the corresponding tensors in the tree-level amplitude. The $A_{6;3}$ term arises from a fermion triangle graph [31]. It violates the axial symmetry, and is proportional to the axial coupling of the Z to the top and bottom quark isodoublet as well as to the top-bottom mass splitting (see section 3.4). The corresponding charges vanish for the photon and the W boson, and this term does not contribute to amplitudes for the latter bosons.

Helicity conservation for massless quarks and leptons ensures that there are only $2^3 = 8$ possible helicity configurations for $e^+e^- \rightarrow \bar{q}q\bar{Q}Q$, namely two choices for each fermion line. Because the electron line couples through the current $\langle 5^\pm | \gamma^\mu | 6^\pm \rangle = \langle 6^\mp | \gamma^\mu | 5^\mp \rangle$, it is trivial to reverse its helicity simply by exchanging 5 and 6 in the partial amplitudes A_6^{tree} and $A_{6;i}$, and exchanging $v_R^e \leftrightarrow v_L^e$ in the prefactors in eqs. (2.3) and (2.6) as discussed above. We can use parity to reverse all helicities simultaneously in the partial amplitudes A_6^{tree} , $A_{6;1}$ and $A_{6;2}$, by complex conjugating all spinor products ($\langle i j \rangle \leftrightarrow [j i]$). The axial vector contribution $A_{6;3}$ is also complex conjugated, but acquires an additional overall minus sign from the γ_5 in the loop. Thus we are left with just two independent helicity configurations, which we may take to be $\mathcal{A}_6(1_q^+, 2_{\bar{Q}}^\pm, 3_Q^\mp, 4_{\bar{q}}^-; 5_e^-, 6_e^+)$ (we shall again suppress the 5, 6 labels below).

The partial amplitudes can be further expressed in terms of ‘primitive amplitudes’ [15]. The primitive amplitudes are gauge-invariant classes of color-stripped amplitudes from which we can build the partial amplitudes. (In ref. [15] the primitive amplitudes were defined to have a fixed ordering of the external legs, but here we extend the notion to mean gauge-invariant color-stripped building-blocks for amplitudes.) It turns out that some signs in the reduction of partial amplitudes to primitive amplitudes depend on which of the two helicity configurations one is considering, so for clarity we shall explicitly list the two cases separately. Although color decompositions do not depend on the helicity choices, these sign differences appear because we have used the symmetries of the primitive amplitudes to reduce the number of independent ones required.

The formulæ for $A_{6;i}(1_q^+, 2_{\bar{Q}}^\pm, 3_Q^\mp, 4_{\bar{q}}^-)$ in terms of the primitive amplitudes are

$$\begin{aligned} A_{6;1}(1_q^+, 2_{\bar{Q}}^\pm, 3_Q^\mp, 4_{\bar{q}}^-) &= A_6^{++}(1, 2, 3, 4) + \frac{n_s - n_f}{N_c} A_6^{s,++}(1, 2, 3, 4) - \frac{n_f}{N_c} A_6^{f,++}(1, 2, 3, 4) \\ &\quad - \frac{2}{N_c^2} (A_6^{++}(1, 2, 3, 4) + A_6^{+-}(1, 3, 2, 4)) + \frac{1}{N_c^2} A_6^{\text{sl}}(2, 3, 1, 4), \\ A_{6;2}(1_q^+, 2_{\bar{Q}}^\pm, 3_Q^\mp, 4_{\bar{q}}^-) &= A_6^{+-}(1, 3, 2, 4) - \frac{n_s - n_f}{N_c} A_6^{s,++}(1, 2, 3, 4) + \frac{n_f}{N_c} A_6^{f,++}(1, 2, 3, 4) \\ &\quad + \frac{1}{N_c^2} (A_6^{+-}(1, 3, 2, 4) + A_6^{++}(1, 2, 3, 4)) - \frac{1}{N_c^2} A_6^{\text{sl}}(2, 3, 1, 4), \end{aligned} \quad (2.7)$$

$$A_{6;3}(1_q^+, 2_{\bar{Q}}^\pm, 3_Q^\mp, 4_{\bar{q}}^-) = A_6^{\text{ax}}(1, 4, 2, 3),$$

where n_s is the number of scalars* ($n_s = 0$ in QCD) and n_f is the number of Dirac fermions. Within the context of supersymmetry decompositions [13,32,12] it is natural to divide the fermion contribution into s and f pieces as we have done here.

* As in refs. [13,15], each scalar here contains four states (to match the four states of Dirac fermions) so that n_s must be divided by two for comparisons to conventional normalizations of scalars.

For the other independent helicity configuration $A_{6;i}(1_q^+, 2_{\bar{Q}}^-, 3_Q^+, 4_{\bar{q}}^-)$, we have,

$$\begin{aligned}
A_{6;1}(1_q^+, 2_{\bar{Q}}^-, 3_Q^+, 4_{\bar{q}}^-) &= A_6^{+-}(1, 2, 3, 4) + \frac{n_s - n_f}{N_c} A_6^{s,+-}(1, 2, 3, 4) - \frac{n_f}{N_c} A_6^{f,+-}(1, 2, 3, 4) \\
&\quad - \frac{2}{N_c^2} (A_6^{+-}(1, 2, 3, 4) + A_6^{++}(1, 3, 2, 4)) - \frac{1}{N_c^2} A_6^{\text{sl}}(3, 2, 1, 4), \\
A_{6;2}(1_q^+, 2_{\bar{Q}}^-, 3_Q^+, 4_{\bar{q}}^-) &= A_6^{++}(1, 3, 2, 4) - \frac{n_s - n_f}{N_c} A_6^{s,+-}(1, 2, 3, 4) + \frac{n_f}{N_c} A_6^{f,+-}(1, 2, 3, 4) \quad (2.8) \\
&\quad + \frac{1}{N_c^2} (A_6^{++}(1, 3, 2, 4) + A_6^{+-}(1, 2, 3, 4)) + \frac{1}{N_c^2} A_6^{\text{sl}}(3, 2, 1, 4), \\
A_{6;3}(1_q^+, 2_{\bar{Q}}^-, 3_Q^+, 4_{\bar{q}}^-) &= -A_6^{\text{ax}}(1, 4, 3, 2).
\end{aligned}$$

Note that A_6^{sl} and A_6^{ax} appear with a different permutation of the arguments, and the opposite sign, compared with the previous helicity structure. The signs in the above expressions also depend on the relative phase conventions of the two helicity amplitudes; we have chosen a convention where $A_6^{\text{tree},+-}(1, 3, 2, 4) = -A_6^{\text{tree},++}(1, 2, 3, 4)$. Of course, consistency between tree and loop amplitudes must be maintained.

A representative diagram for the primitive amplitudes $A_6^{s,\pm\pm}(1, 2, 3, 4)$ and $A_6^{f,\pm\pm}(1, 2, 3, 4)$, corresponding to those terms in the partial amplitudes proportional to the number of fermions n_f , is depicted in fig. 1. There are only two such diagrams. The ‘parent’ pentagon diagram for the leading-color helicity amplitude $A_6^{+\pm}(1, 2, 3, 4)$ is depicted in fig. 2. (By a ‘parent’ diagram we mean a diagram from which all other diagrams in the set can be obtained via a continuous ‘pinching’ process, in which two lines attached to the loop are brought together to a four-point interaction — if such an interaction exists — or further pulled out from the loop, and left as the branches of a tree attached to the loop.) The parent box and triangle diagrams for the subleading-color primitive amplitude $A_6^{\text{sl}}(1, 2, 3, 4)$ are depicted in fig. 3. (We combine the triangle-parent contributions with the box-parent contributions because the former are so simple, and the two have an identical color structure.) The fermion-loop triangle diagram, proportional to the axial coupling of the Z to quarks, is shown in fig. 4. We neglect the u, d, s, c quark masses, and so only the t, b quark pair survives an isodoublet cancellation in the loop, thanks to its large mass splitting.

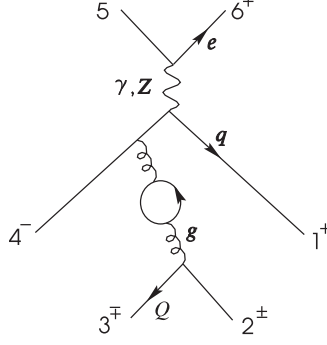


Figure 1. One of the two fermion bubble diagrams contributing to $A_6^{s,+ \pm}$ and $A_6^{f,+ \pm}$.

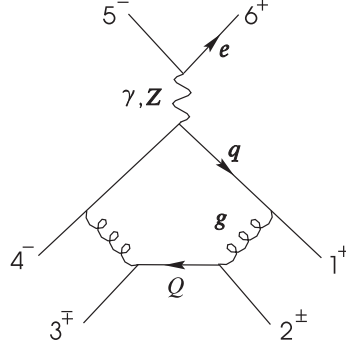


Figure 2. The parent diagram for the leading-color helicity amplitudes $A_6^{+ \pm}$.

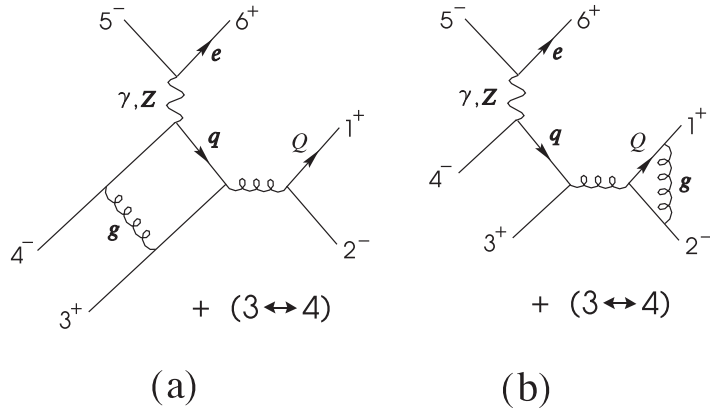


Figure 3. The diagrams for the subleading-color component A_6^{sl} can be divided into (a) those with a parent box diagram), and (b) those with a parent triangle diagram. Note that the labelling of legs is different from that in the leading-color diagrams.

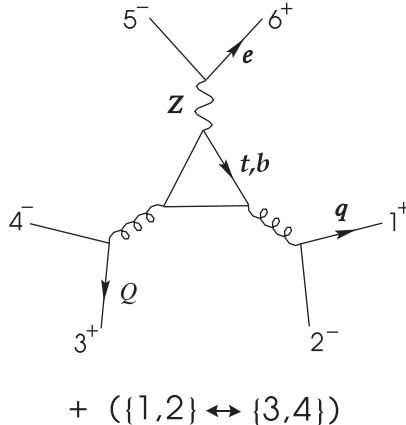


Figure 4. Triangle diagram for the amplitude component A_6^{ax} , proportional to the axial coupling of the Z to quarks.

Formulas (2.3) and (2.6) apply to the case of unequal quark flavors, $q \neq Q$. The equal flavor amplitude may be obtained from the unequal-flavor formula by subtracting the same formula with q and Q exchanged (*or* \bar{q} and \bar{Q} exchanged, but not both), and then setting $Q = q$ in all the coupling constant prefactors. (Equal-flavor cross sections also require an identical-particle factor in the phase-space measure, which is $(\frac{1}{2})^2$ for $e^+e^- \rightarrow \bar{q}q\bar{q}q$.)

The virtual part of the next-to-leading order correction to the parton-level cross-section is given by

$$d\sigma_6^{\text{NLO,virtual}} = 2 \sum_{\text{colors}} \text{Re}[\mathcal{A}_6^{\text{tree}} * \mathcal{A}_6^{1\text{-loop}}]. \quad (2.9)$$

It is a straightforward exercise (which we leave to the reader) to evaluate this color sum in terms of partial amplitudes.

3. The Amplitudes

In constructing the amplitudes presented here, we use two basic analytic properties: that their imaginary (absorptive) parts be determined from the Cutkosky rules [20], and that they factorize on particle poles. These analytic properties of amplitudes have, of course, played an important role in field theory for many decades; we make use of recent developments which allow us to obtain complete amplitudes with no subtractions. In order to maximize the efficiency of the computation it is useful to perform the computation in the manner described in ref. [12]. Due to the complexity of the kinematics for the processes presented here, further techniques are required to minimize the appearance of undesired spurious poles; these will be discussed in ref. [9].

The primitive amplitudes A_6^f and A_6^s are proportional to tree amplitudes and are given by

$$\begin{aligned} A_6^{s,+ \pm}(1, 2, 3, 4) &= c_\Gamma A_6^{\text{tree}}(1_q^+, 2_{\bar{Q}}^\pm, 3_Q^\mp, 4_{\bar{q}}; 5_{\bar{e}}^-, 6_e^+) \left[-\frac{1}{3\epsilon} \left(\frac{\mu^2}{-s_{23}} \right)^\epsilon - \frac{8}{9} \right], \\ A_6^{f,+ \pm}(1, 2, 3, 4) &= c_\Gamma A_6^{\text{tree}}(1_q^+, 2_{\bar{Q}}^\pm, 3_Q^\mp, 4_{\bar{q}}; 5_{\bar{e}}^-, 6_e^+) \left[\frac{1}{\epsilon} \left(\frac{\mu^2}{-s_{23}} \right)^\epsilon + 2 \right], \end{aligned} \quad (3.1)$$

where A_6^{tree} is given below,

$$c_\Gamma = \frac{1}{(4\pi)^{2-\epsilon}} \frac{\Gamma(1+\epsilon)\Gamma^2(1-\epsilon)}{\Gamma(1-2\epsilon)}, \quad (3.2)$$

and $D = 4 - 2\epsilon$.

The contribution A_6^{ax} is finite (see below). It is convenient to decompose the remaining primitive amplitudes into divergent (V) and finite (F) pieces,

$$A_6^\alpha = c_\Gamma \left[A_6^{\text{tree}, \alpha} V^\alpha + i F^\alpha \right], \quad (3.3)$$

where

$$\alpha = \{++, \quad +-, \quad \text{sl}\} \quad (3.4)$$

labels the primitive amplitude under discussion. The quantities $A_6^{\text{tree}, + \pm}$ coincide with the true tree partial amplitudes appearing in eq. (2.3),

$$A_6^{\text{tree}}(1_q^+, 2_{\bar{Q}}^\pm, 3_Q^\mp, 4_{\bar{q}}; 5_{\bar{e}}^-, 6_e^+) = A_6^{\text{tree}, + \pm}(1, 2, 3, 4). \quad (3.5)$$

(We continue to omit the arguments of the primitive amplitudes corresponding to the lepton pair.) We express the amplitudes in terms of the spinor products (2.2), the Lorentz products $s_{ij} = (k_i + k_j)^2$ and $t_{ijm} = (k_i + k_j + k_m)^2$, and the following combinations of kinematic invariants,

$$\begin{aligned} \delta_{12} &= s_{12} - s_{34} - s_{56}, & \delta_{34} &= s_{34} - s_{56} - s_{12}, & \delta_{56} &= s_{56} - s_{12} - s_{34}, \\ \Delta_3 &= s_{12}^2 + s_{34}^2 + s_{56}^2 - 2s_{12}s_{34} - 2s_{34}s_{56} - 2s_{56}s_{12}. \end{aligned} \quad (3.6)$$

The latter quantity is the negative of the Gram determinant associated with the set of massive momenta $\{k_1 + k_2, k_3 + k_4, k_5 + k_6\}$.

The amplitudes we present are bare ones, i.e., no ultra-violet subtraction has been performed. To obtain the renormalized amplitudes in an $\overline{\text{MS}}$ -type subtraction scheme, one should subtract the quantity

$$c_\Gamma N_c g^2 \left[\frac{1}{\epsilon} \left(\frac{11}{3} - \frac{2}{3} \frac{n_f}{N_c} - \frac{1}{3} \frac{n_s}{N_c} \right) \right] \mathcal{A}_6^{\text{tree}}, \quad (3.7)$$

from the the amplitude (2.6).

We quote the results in the FDH scheme [30,28], but these may easily be converted to the 't Hooft-Veltman scheme; to do so one would add the quantity

$$-c_\Gamma N_c g^2 \left(\frac{2}{3} - \frac{1}{N_c^2} \right) \mathcal{A}_6^{\text{tree}} \quad (3.8)$$

to the amplitude (2.6) and change the coupling constant from the non-standard $\alpha_{\overline{DR}}$ to the standard $\alpha_{\overline{MS}}$. The conversion between the various schemes is discussed in refs. [29].

3.1 The Helicity Configuration $q^+\bar{Q}^+Q^-\bar{q}^-$

We first give the primitive amplitude $A_6^{++}(1, 2, 3, 4)$ which contributes to the leading color part of $A_{6;1}(1_q^+, 2_{\bar{Q}}^+, 3_Q^-, 4_{\bar{q}}^-; 5_{\bar{e}}^-, 6_e^+)$. This amplitude is odd under a ‘flip symmetry’, which is the combined operation of a permutation and spinor-product complex conjugation:

$$\text{flip:} \quad 1 \leftrightarrow 4, \quad 2 \leftrightarrow 3, \quad 5 \leftrightarrow 6, \quad \langle a b \rangle \leftrightarrow [a b], \quad \langle a^- | b | c^- \rangle \leftrightarrow \langle a^+ | b | c^+ \rangle = \langle c^- | b | a^- \rangle. \quad (3.9)$$

The corresponding tree amplitude for this helicity configuration is

$$A_6^{\text{tree}, ++}(1, 2, 3, 4) = i \frac{[1\,2] \langle 5\,4 \rangle \langle 3|(1+2)|6 \rangle}{s_{23}s_{56}t_{123}} + i \frac{\langle 3\,4 \rangle [6\,1] \langle 5|(3+4)|2 \rangle}{s_{23}s_{56}t_{234}}. \quad (3.10)$$

We have

$$\begin{aligned} V^{++}(1, 2, 3, 4) = & -\frac{1}{\epsilon^2} \left(\left(\frac{\mu^2}{-s_{12}} \right)^\epsilon + \left(\frac{\mu^2}{-s_{34}} \right)^\epsilon \right) + \frac{2}{3\epsilon} \left(\frac{\mu^2}{-s_{23}} \right)^\epsilon - \frac{3}{2} \ln \left(\frac{-s_{23}}{-s_{56}} \right) + \frac{10}{9}, \quad (3.11) \\ F^{++}(1, 2, 3, 4) = & \left(\frac{\langle 3|(1+2)|6 \rangle^2}{\langle 2\,3 \rangle [5\,6] t_{123} \langle 1|(2+3)|4 \rangle} - \frac{[1\,2]^2 \langle 4\,5 \rangle^2}{[2\,3] \langle 5\,6 \rangle t_{123} \langle 4|(2+3)|1 \rangle} \right) \\ & \times \left[\text{LS}_{-1} \left(\frac{-s_{12}}{-t_{123}}, \frac{-s_{23}}{-t_{123}} \right) + \widetilde{\text{LS}}_{-1}^{2mh}(s_{34}, t_{123}; s_{12}, s_{56}) \right] \\ & - 2 \frac{\langle 3|(1+2)|6 \rangle}{[5\,6] \langle 1|(2+3)|4 \rangle} \left[\frac{\langle 1|(2+3)|6 \rangle [1\,2] \text{L}_0 \left(\frac{-s_{23}}{-t_{123}} \right)}{t_{123}} + \frac{\langle 3|4|6 \rangle \text{L}_0 \left(\frac{-s_{56}}{-t_{123}} \right)}{t_{123}} \right] \\ & - \frac{1}{2} \frac{1}{\langle 2\,3 \rangle [5\,6] t_{123} \langle 1|(2+3)|4 \rangle} \left[\left(\langle 3|2|1 \rangle \langle 1|(2+3)|6 \rangle \right)^2 \frac{\text{L}_1 \left(\frac{-t_{123}}{-s_{23}} \right)}{s_{23}^2} + \langle 3|4|6 \rangle^2 t_{123}^2 \frac{\text{L}_1 \left(\frac{-s_{56}}{-t_{123}} \right)}{t_{123}^2} \right] \\ & - \text{flip}, \quad (3.12) \end{aligned}$$

where ‘flip’ is to be applied to all the preceding terms in F^{++} .

3.2 The Helicity Configuration $q^+\bar{Q}^-Q^+\bar{q}^-$

We now give the result for $A_6^{+-}(1, 2, 3, 4)$, which contributes to the leading color part of the partial amplitude $A_{6;1}(1_q^+, 2_{\bar{Q}}^-, 3_Q^+, 4_{\bar{q}}^-; 5_{\bar{e}}^-, 6_e^+)$. This amplitude is odd under the same flip symmetry (3.9) as A_6^{++} . The tree amplitude is

$$A_6^{\text{tree}, +-}(1, 2, 3, 4) = -i \frac{[1\,3] \langle 5\,4 \rangle \langle 2|(1+3)|6 \rangle}{s_{23}s_{56}t_{123}} - i \frac{\langle 2\,4 \rangle [6\,1] \langle 5|(2+4)|3 \rangle}{s_{23}s_{56}t_{234}}. \quad (3.13)$$

Note that $A_6^{\text{tree}, +-}(1, 2, 3, 4) = -A_6^{\text{tree}, ++}(1, 3, 2, 4)$.

For the one-loop contributions we have

$$V^{+-}(1, 2, 3, 4) = -\frac{1}{\epsilon^2} \left(\left(\frac{\mu^2}{-s_{12}} \right)^\epsilon + \left(\frac{\mu^2}{-s_{34}} \right)^\epsilon \right) + \frac{2}{3\epsilon} \left(\frac{\mu^2}{-s_{23}} \right)^\epsilon - \frac{3}{2} \ln \left(\frac{-s_{23}}{-s_{56}} \right) + \frac{10}{9}. \quad (3.14)$$

Note that $V^{+-}(1, 2, 3, 4) = V^{++}(1, 2, 3, 4)$. The finite part is

$$\begin{aligned} F^{+-}(1, 2, 3, 4) = & \left(-\frac{[13]^2 \langle 45 \rangle^2}{[23] \langle 56 \rangle t_{123} \langle 4|(2+3)|1\rangle} + \frac{\langle 12 \rangle^2 \langle 3|(1+2)|6 \rangle^2}{\langle 23 \rangle [56] t_{123} \langle 13 \rangle^2 \langle 1|(2+3)|4 \rangle} \right) \text{Ls}_{-1} \left(\frac{-s_{12}}{-t_{123}}, \frac{-s_{23}}{-t_{123}} \right) \\ & + \left(-\frac{[13]^2 \langle 45 \rangle^2}{[23] \langle 56 \rangle t_{123} \langle 4|(2+3)|1\rangle} + \frac{\langle 3|(1+2)|6 \rangle^2 \langle 2|(1+3)|4 \rangle^2}{\langle 23 \rangle [56] t_{123} \langle 1|(2+3)|4 \rangle \langle 3|(1+2)|4 \rangle^2} \right) \widetilde{\text{Ls}}_{-1}^{2mh}(s_{34}, t_{123}; s_{12}, s_{56}) \\ & + \left[\frac{1}{2} \frac{(s_{12} - s_{34}) \langle 51 \rangle \langle 5|(3+4)|2 \rangle \langle 1|(2+4)|3 \rangle}{\langle 56 \rangle \langle 1|(2+3)|4 \rangle \langle 1|(3+4)|2 \rangle^2} - \frac{1}{2} \frac{(s_{12} - s_{34}) [23] \langle 51 \rangle \langle 52 \rangle}{\langle 56 \rangle \langle 1|(2+3)|4 \rangle \langle 1|(3+4)|2 \rangle} \right. \\ & - \frac{1}{2} \frac{(t_{134} - t_{234}) [34] \langle 51 \rangle \langle 54 \rangle}{\langle 56 \rangle \langle 1|(2+3)|4 \rangle \langle 1|(3+4)|2 \rangle} - \frac{[12] \langle 51 \rangle \langle 52 \rangle \langle 1|(2+4)|3 \rangle}{\langle 56 \rangle \langle 1|(2+3)|4 \rangle \langle 1|(3+4)|2 \rangle} \\ & + \frac{1}{2} \frac{\langle 51 \rangle [62] \langle 1|(2+4)|3 \rangle (t_{234} - 2s_{34})}{\langle 1|(2+3)|4 \rangle \langle 1|(3+4)|2 \rangle^2} + \frac{1}{2} \frac{\langle 5|(1+2)|6 \rangle \langle 1|(2+4)|3 \rangle}{\langle 1|(2+3)|4 \rangle \langle 1|(3+4)|2 \rangle} \\ & - \frac{\langle 1|(2+4)|3 \rangle (s_{12} \delta_{12} (\langle 51|6 \rangle - \langle 52|6 \rangle) - \delta_{56} (\langle 51|2 \rangle \langle 2|5|6 \rangle - \langle 5|6|1 \rangle \langle 1|2|6 \rangle))}{\langle 1|(2+3)|4 \rangle \langle 1|(3+4)|2 \rangle \Delta_3} \\ & \left. + \frac{1}{2} \frac{\langle 2|(1+4)|3 \rangle \langle 5|(1+2)|6 \rangle \delta_{56}}{\langle 1|(2+3)|4 \rangle \Delta_3} \right] I_3^{\text{3m}}(s_{12}, s_{34}, s_{56}) \\ & + \frac{[13] \langle 12 \rangle \langle 3|(1+2)|6 \rangle^2}{[56] t_{123} \langle 13 \rangle \langle 3|(1+2)|4 \rangle} \frac{\text{L}_0 \left(\frac{-t_{123}}{-s_{12}} \right)}{s_{12}} - \frac{1}{2} \frac{[13]^2 \langle 23 \rangle \langle 1|(2+3)|6 \rangle^2}{[56] t_{123} \langle 1|(2+3)|4 \rangle} \frac{\text{L}_1 \left(\frac{-t_{123}}{-s_{23}} \right)}{s_{23}^2} \\ & + \frac{[13] \langle 1|(2+3)|6 \rangle \langle 2|(1+3)|6 \rangle}{[56] t_{123} \langle 1|(2+3)|4 \rangle} \frac{\text{L}_0 \left(\frac{-t_{123}}{-s_{23}} \right)}{s_{23}} + \frac{[13] \langle 12 \rangle \langle 1|(2+3)|6 \rangle \langle 3|(1+2)|6 \rangle}{[56] t_{123} \langle 13 \rangle \langle 1|(2+3)|4 \rangle} \frac{\text{L}_0 \left(\frac{-t_{123}}{-s_{23}} \right)}{s_{23}} \\ & - \frac{1}{2} \frac{[64]^2 \langle 42 \rangle^2 t_{123}}{\langle 23 \rangle [56] \langle 1|(2+3)|4 \rangle} \frac{\text{L}_1 \left(\frac{-s_{56}}{-t_{123}} \right)}{t_{123}^2} - \frac{[64]^2 \langle 42 \rangle t_{123}}{[56] \langle 1|(2+3)|4 \rangle \langle 3|(1+2)|4 \rangle} \frac{\text{L}_0 \left(\frac{-t_{123}}{-s_{56}} \right)}{s_{56}} \\ & - 2 \frac{[64] \langle 42 \rangle \langle 2|(1+3)|6 \rangle}{\langle 23 \rangle [56] \langle 1|(2+3)|4 \rangle} \frac{\text{L}_0 \left(\frac{-t_{123}}{-s_{56}} \right)}{s_{56}} \\ & + \frac{1}{\langle 3|(1+2)|4 \rangle \langle 1|(3+4)|2 \rangle \Delta_3} \left[(s_{12} - s_{34}) \left(\frac{\langle 12 \rangle [61] [62] t_{123}}{[56]} + \frac{[12] \langle 51 \rangle \langle 52 \rangle t_{124}}{\langle 56 \rangle} \right) \right. \\ & + (2s_{12} - \delta_{56}) \langle 52 \rangle \langle 1|(3+4)|2 \rangle [16] \\ & + ((s_{13} + s_{23})(s_{23} + s_{24}) - s_{12}(s_{12} + s_{23} - s_{14})) \langle 5|1|6 \rangle \\ & \left. + ((s_{14} + s_{24})(s_{13} + s_{14}) - s_{12}(s_{12} - s_{23} + s_{14})) \langle 5|2|6 \rangle \right] \ln \left(\frac{-s_{12}}{-s_{56}} \right) \\ & - \text{flip}, \end{aligned} \quad (3.15)$$

where ‘flip’ is to be applied to all the preceding terms in F^{+-} .

3.3 Subleading Color Primitive Amplitude

Here we give the primitive amplitude $A_6^{\text{sl}}(1, 2, 3, 4)$, which contributes only at subleading order

in N_c . The “tree amplitude” appearing in eq. (3.3) is

$$A_6^{\text{tree,sl}}(1, 2, 3, 4) = i \frac{[1\,3] \langle 5\,4 \rangle \langle 2|(1+3)|6 \rangle}{s_{12}s_{56}t_{123}} - i \frac{\langle 2\,4 \rangle [6\,3] \langle 5|(2+4)|1 \rangle}{s_{12}s_{56}t_{124}}. \quad (3.16)$$

Note that $A_6^{\text{tree,sl}}(2, 3, 1, 4) = -A_6^{\text{tree,}++}(1, 2, 3, 4)$.

For the subleading-color primitive amplitude, it is convenient to introduce an ‘exchange’ operation where the 5, 6 fermion pair is exchanged with the 1, 2 fermion pair,

$$\text{exchange:} \quad 1 \leftrightarrow 6, \quad 2 \leftrightarrow 5. \quad (3.17)$$

The box-parent part of A_6^{sl} is even under this exchange. It is also convenient to define a symmetry operation ‘flip_{sl}’ (distinct from the leading-color ‘flip’),

$$\text{flip}_{\text{sl}}: \quad 1 \leftrightarrow 5, \quad 2 \leftrightarrow 6, \quad 3 \leftrightarrow 4, \quad \langle a\,b \rangle \leftrightarrow [a\,b], \quad \langle a^-|b|c^- \rangle \leftrightarrow \langle a^+|b|c^+ \rangle = \langle c^-|b|a^- \rangle. \quad (3.18)$$

The singular contribution is

$$V^{\text{sl}}(1, 2, 3, 4) = \left[-\frac{1}{\epsilon^2} \left(\frac{\mu^2}{-s_{34}} \right)^\epsilon - \frac{3}{2\epsilon} \left(\frac{\mu^2}{-s_{34}} \right)^\epsilon - 4 \right] + \left[-\frac{1}{\epsilon^2} \left(\frac{\mu^2}{-s_{12}} \right)^\epsilon - \frac{3}{2\epsilon} \left(\frac{\mu^2}{-s_{12}} \right)^\epsilon - \frac{7}{2} \right], \quad (3.19)$$

where the first bracket is from the ‘box parent’ graphs in fig. 3a and the second bracket is from the ‘triangle parent’ graphs in fig. 3b. In fact, the entire contribution from the triangle parent diagrams

is contained in the second bracket. The finite contribution is

$$\begin{aligned}
F^{\text{sl}}(1, 2, 3, 4) = & \left[\frac{[1\,3]^2 \langle 4\,5 \rangle^2}{[1\,2] \langle 5\,6 \rangle t_{123} \langle 4|(1+2)|3 \rangle} - \frac{\langle 3|(1+2)|6 \rangle^2 \langle 2|(1+3)|4 \rangle^2}{\langle 1\,2 \rangle [5\,6] t_{123} \langle 3|(1+2)|4 \rangle^3} \right] \widetilde{\text{LS}}_{-1}^{2mh}(s_{34}, t_{123}; s_{12}, s_{56}) \\
& + T I_3^{\text{3m}}(s_{12}, s_{34}, s_{56}) + \left[\frac{1}{2} \frac{[6\,4]^2 \langle 4\,2 \rangle^2 t_{123}}{\langle 1\,2 \rangle [5\,6] \langle 3|(1+2)|4 \rangle} \frac{\text{L}_1\left(\frac{-s_{56}}{-t_{123}}\right)}{t_{123}^2} + 2 \frac{[6\,4] \langle 4\,2 \rangle \langle 2|(1+3)|6 \rangle}{\langle 1\,2 \rangle [5\,6] \langle 3|(1+2)|4 \rangle} \frac{\text{L}_0\left(\frac{-t_{123}}{-s_{56}}\right)}{s_{56}} \right. \\
& - \frac{\langle 2\,3 \rangle \langle 2\,4 \rangle [6\,4]^2 t_{123}}{\langle 1\,2 \rangle [5\,6] \langle 3|(1+2)|4 \rangle^2} \frac{\text{L}_0\left(\frac{-t_{123}}{-s_{56}}\right)}{s_{56}} - \frac{1}{2} \frac{\langle 2\,3 \rangle [6\,4] \langle 2|(1+3)|6 \rangle}{\langle 1\,2 \rangle [5\,6] \langle 3|(1+2)|4 \rangle^2} \ln\left(\frac{-t_{123}}{-s_{56}}\right) \\
& - \frac{3}{4} \frac{\langle 2|(1+3)|6 \rangle^2}{\langle 1\,2 \rangle [5\,6] t_{123} \langle 3|(1+2)|4 \rangle} \ln\left(\frac{-t_{123}}{-s_{56}}\right) - \text{flip_sl} \left. \right] \\
& + \left[\ln\left(\frac{-s_{12}}{-s_{34}}\right) \left(\frac{3}{2} \frac{[1\,2]}{\langle 3|(1+2)|4 \rangle \Delta_3^2} ([5\,6] \langle 2\,5 \rangle^2 \delta_{34} \delta_{56} - 2 \langle 1\,2 \rangle^2 \langle 5\,6 \rangle [6\,1]^2 \delta_{12} + 4 \langle 1\,2 \rangle s_{56} \langle 5\,2 \rangle [6\,1] \delta_{56}) \right. \right. \\
& - \frac{1}{2} \frac{[1\,2] \langle 2\,5 \rangle}{\langle 3|(1+2)|4 \rangle \langle 5\,6 \rangle \Delta_3} (\langle 5\,2 \rangle (s_{12} - s_{34}) - 2 \langle 5\,6 \rangle [6\,1] \langle 1\,2 \rangle) \\
& + \frac{3}{2} \frac{t_{123}}{\langle 3|(1+2)|4 \rangle \Delta_3^2} (\langle 5\,2 \rangle [1\,6] (\delta_{34} \delta_{56} + 2 s_{12} \delta_{12}) + 2 ([1\,2] [5\,6] \langle 2\,5 \rangle^2 + \langle 1\,2 \rangle \langle 5\,6 \rangle [6\,1]^2) \delta_{56}) \\
& - \frac{1}{2} \frac{t_{123}}{\langle 3|(1+2)|4 \rangle \Delta_3} \left(\langle 5\,2 \rangle [1\,6] - \frac{[1\,2] \langle 2\,5 \rangle^2}{\langle 5\,6 \rangle} - \frac{\langle 1\,2 \rangle [6\,1]^2}{[5\,6]} \right) \\
& + \left(-\frac{[1\,2] [6\,4] \langle 3\,2 \rangle}{\langle 3|(1+2)|4 \rangle^2 \Delta_3} + \frac{\langle 5|(2+3)|1 \rangle}{\langle 5\,6 \rangle \langle 3|(1+2)|4 \rangle \Delta_3} \right) (\langle 5\,2 \rangle \delta_{56} - 2 \langle 5|(3+4)|1 \rangle \langle 1\,2 \rangle) \\
& - \frac{[6\,4] \langle 3\,2 \rangle t_{123}}{[5\,6] \langle 3|(1+2)|4 \rangle^2 \Delta_3} ([1\,6] \delta_{56} - 2 \langle 2|(3+4)|6 \rangle [1\,2]) \\
& + \frac{4}{\langle 3|(1+2)|4 \rangle \Delta_3} (\langle 5\,4 \rangle [4\,1] \langle 2|(1+3)|6 \rangle + [6\,3] \langle 2\,3 \rangle \langle 5|(2+4)|1 \rangle) \\
& + 2 \frac{[6\,4] \langle 4\,2 \rangle}{\langle 1\,2 \rangle [5\,6] \langle 3|(1+2)|4 \rangle \Delta_3} (-2 \langle 2|5|6 \rangle \delta_{56} + \langle 2|(3+4)|6 \rangle \delta_{34}) \\
& - 2 \frac{\langle 5\,2 \rangle}{\langle 1\,2 \rangle \langle 5\,6 \rangle \langle 3|(1+2)|4 \rangle \Delta_3} \delta_{34} (\langle 5\,3 \rangle [3\,4] \langle 4\,2 \rangle + \langle 5\,4 \rangle [4\,1] \langle 1\,2 \rangle - \langle 5|(1+2)|3 \rangle \langle 3\,2 \rangle) \\
& - \frac{[6\,4] \langle 2|(1+3)|6 \rangle \langle 2^-(5+6)(1+2)|3^+ \rangle}{\langle 1\,2 \rangle [5\,6] t_{123} \langle 3|(1+2)|4 \rangle^2} + \frac{1}{2} \frac{\langle 2\,3 \rangle [4\,6] \langle 2|(1+3)|6 \rangle}{\langle 1\,2 \rangle [5\,6] \langle 3|(1+2)|4 \rangle^2} \\
& - \frac{1}{4} \frac{\langle 2|(1+3)|6 \rangle^2}{\langle 1\,2 \rangle [5\,6] t_{123} \langle 3|(1+2)|4 \rangle} + \frac{\langle 5\,2 \rangle (\langle 4\,5 \rangle \langle 2|(1+3)|4 \rangle - \langle 2\,5 \rangle t_{123})}{\langle 1\,2 \rangle \langle 5\,6 \rangle t_{123} \langle 3|(1+2)|4 \rangle} \left. \right) - \text{flip_sl} \left. \right] \\
& - \frac{1}{2} \frac{(t_{123} \delta_{34} + 2 s_{12} s_{56})}{\langle 3|(1+2)|4 \rangle \Delta_3} \left(\frac{[6\,1]^2}{[1\,2] [5\,6]} + \frac{\langle 5\,2 \rangle^2}{\langle 1\,2 \rangle \langle 5\,6 \rangle} \right) + (t_{123} - t_{124}) \frac{[6\,1] \langle 5\,2 \rangle}{\langle 3|(1+2)|4 \rangle \Delta_3} \\
& + \text{exchange}, \tag{3.20}
\end{aligned}$$

where ‘exchange’ is to be applied to all the preceding terms in F^{sl} , but ‘flip_sl’ is to be applied only to the terms inside the brackets ([]) in which it appears. The three-mass triangle coefficient T is

given by

$$\begin{aligned}
T = & 3s_{34}(t_{123}\delta_{34} + 2s_{12}s_{56}) \frac{([12] \langle 25 \rangle^2 [56] + \langle 56 \rangle [61]^2 \langle 12 \rangle)}{\langle 3|(1+2)|4\rangle \Delta_3^2} - 6s_{12}s_{56}s_{34} \langle 52 \rangle [61] \frac{(t_{123} - t_{124})}{\langle 3|(1+2)|4\rangle \Delta_3^2} \\
& - \frac{t_{123}}{\langle 3|(1+2)|4\rangle \Delta_3} (\langle 52 \rangle [61] (s_{56} + s_{12} + s_{34}) + [12] \langle 25 \rangle^2 [56] + \langle 56 \rangle [61]^2 \langle 12 \rangle) \\
& - \frac{\langle 5|(2+3)|1\rangle}{\langle 3|(1+2)|4\rangle \Delta_3} ([65] \langle 52 \rangle \delta_{56} - [61] \langle 12 \rangle \delta_{12}) - \frac{[12] \langle 56 \rangle \langle 2|(3+4)|6\rangle^2}{\langle 3|(1+2)|4\rangle \Delta_3} \\
& - \frac{\langle 23 \rangle [64]}{\langle 3|(1+2)|4\rangle^2 \Delta_3} (\langle 56 \rangle \delta_{56} ([61] t_{123} - [65] \langle 52 \rangle [21]) - [12] \delta_{12} (\langle 25 \rangle t_{123} - \langle 21 \rangle [16] \langle 65 \rangle)) \\
& - \frac{\langle 23 \rangle [64] \langle 5|(2+3)|1\rangle}{\langle 3|(1+2)|4\rangle^2} - \frac{1}{2} (t_{123}\delta_{34} + 2s_{12}s_{56}) \frac{\langle 23 \rangle^2 [64]^2}{\langle 12 \rangle [56] \langle 3|(1+2)|4\rangle^3} \\
& - 2([65] \langle 52 \rangle \delta_{56} - [61] \langle 12 \rangle \delta_{12}) \frac{[63] \langle 24 \rangle}{\langle 12 \rangle [56] \Delta_3} \\
& + 2(-\langle 2|3|4\rangle \langle 4|5|6\rangle \delta_{56} + \langle 2|1|3\rangle \langle 3|4|6\rangle \delta_{12} + \langle 2|(1+3)|6\rangle s_{34} \delta_{34}) \frac{\langle 2|(1+3)|6\rangle}{\langle 12 \rangle [56] \langle 3|(1+2)|4\rangle \Delta_3} \\
& + 4 \frac{\langle 2|(1+3)|6\rangle \langle 5|(2+3)|1\rangle s_{34}}{\langle 3|(1+2)|4\rangle \Delta_3} - (t_{123}\delta_{34} + 2s_{12}s_{56}) \frac{\langle 2|(1+3)|6\rangle [14] \langle 35 \rangle}{s_{12}s_{56} \langle 3|(1+2)|4\rangle^2} \\
& + 2(-[12] \langle 23 \rangle [34] \langle 45 \rangle + \langle 56 \rangle [64] \langle 43 \rangle [31] + \langle 5|(2+3)|1\rangle s_{34}) \frac{\langle 2|(1+3)|6\rangle}{s_{12}s_{56} \langle 3|(1+2)|4\rangle} \\
& - \frac{1}{2} (t_{123}\delta_{34} + 2s_{12}s_{56}) \frac{[16] \langle 25 \rangle}{s_{12}s_{56} \langle 3|(1+2)|4\rangle} \\
& - \frac{1}{2} \frac{(t_{123} - t_{124})}{s_{12}s_{56} \langle 3|(1+2)|4\rangle} (2 \langle 2|(1+3)|6\rangle (\langle 5|3|1\rangle - \langle 5|4|1\rangle) \\
& \quad + (\langle 2|3|6\rangle - \langle 2|4|6\rangle) \langle 5|(2+4)|1\rangle + [61] \langle 25 \rangle \delta_{34}) \\
& + \left(-\langle 5|3|1\rangle + \langle 5|4|1\rangle + \frac{1}{2} (t_{123} - t_{124}) \left(\frac{[14] \langle 35 \rangle}{\langle 3|(1+2)|4\rangle} + \frac{[13] \langle 45 \rangle}{\langle 4|(1+2)|3\rangle} \right) \right) \frac{[36] \langle 24 \rangle}{s_{12}s_{56}} \\
& - (4 \langle 2|(1+3)|6\rangle - \langle 2|3|6\rangle + \langle 2|4|6\rangle) \frac{[13] \langle 45 \rangle}{s_{12}s_{56}}.
\end{aligned} \tag{3.21}$$

3.4 Axial Vector Contribution

The primitive amplitude $A_6^{\text{ax}}(1, 2, 3, 4)$ is unique in that neither of the external quark pairs couples directly to the vector boson; instead they couple through the fermion-loop triangle diagram shown in fig. 4. The contribution to the amplitude (2.6) vanishes when the vector boson is a photon (by Furry's theorem, i.e. charge conjugation invariance). The Z contribution is proportional to the axial vector coupling of the Z to the quarks in the loop. As the u, d, s, c quark masses may be neglected, only the t, b quark pair survives an isodoublet cancellation in the loop, due to its large mass splitting. We use the results of ref. [31] to obtain this contribution; that paper presents the fully off-shell Zgg vertex, and we need only contract it with the three fermion currents. The

infrared- and ultraviolet-finite result is

$$A_6^{\text{ax}}(1, 2, 3, 4) = -\frac{2i}{(4\pi)^2} \frac{f(m_t; s_{12}, s_{34}, s_{56}) - f(m_b; s_{12}, s_{34}, s_{56})}{s_{56}} \left(\frac{[6\,3] \langle 4\,2 \rangle \langle 2\,5 \rangle}{\langle 1\,2 \rangle} - \frac{[6\,1] [1\,3] \langle 4\,5 \rangle}{[1\,2]} \right) + (1 \leftrightarrow 3, \, 2 \leftrightarrow 4) , \quad (3.22)$$

where the integral $f(m)$ is defined in the appendix. We need only the large mass expansion (for $m = m_t$) and the $m = 0$ limit (for $m = m_b$) of this integral; these are presented in the appendix.

4. Summary and Conclusions

In this paper we presented all one-loop four-quark amplitudes which enter into the computation of the next-to-leading order QCD corrections to $e^+e^- \rightarrow (\gamma^*, Z) \rightarrow 4$ jets. The two-quark two-gluon amplitudes will be presented elsewhere [8,9]. We obtained the amplitudes by demanding that their functional forms satisfy unitarity and factorization. We also used a color decomposition and a helicity basis to express the amplitudes in a compact form. This way of obtaining amplitudes is significantly more efficient than using Feynman diagrams, since previously computed amplitudes are used to construct new ones. These amplitudes can be incorporated into numerical jet programs, which should lead to an improved knowledge of the QCD background to searches for new physics in various processes. Indeed, the leading-in- N_c parts of the contributions presented here, together with those for two quarks and two gluons [8,9] have already been inserted into one such program for four-jet production in e^+e^- annihilation [10].

Acknowledgements

L.D. thanks Adrian Signer for useful discussions. L.D. and D.A.K. are grateful for the support of NATO Collaborative Research Grant CRG-921322. S.W. acknowledges the support of the Studienstiftung des deutschen Volkes and of the CEA, under CFR #161635.

Appendix I. Integral Functions

We collect here the integral functions appearing in the text, which contain all logarithms and dilogarithms present in the amplitudes. Except for the contribution of the top quark to the fermion triangle loop in A_6^{ax} , all internal lines are taken to be massless. The following functions already appear in the evaluation of pentagon loop integrals where all external legs are massless, and of box

integrals with one external mass, e.g. as occur in the one-loop five-gluon amplitudes [13]:

$$\begin{aligned} L_0(r) &= \frac{\ln(r)}{1-r}, & L_1(r) &= \frac{L_0(r) + 1}{1-r}, \\ L_{-1}(r_1, r_2) &= \text{Li}_2(1-r_1) + \text{Li}_2(1-r_2) + \ln r_1 \ln r_2 - \frac{\pi^2}{6}, \end{aligned} \quad (\text{I.1})$$

where the dilogarithm is

$$\text{Li}_2(x) = - \int_0^x dy \frac{\ln(1-y)}{y}. \quad (\text{I.2})$$

The function L_{-1} is simply related to the scalar box integral with one external mass, evaluated in six space-time dimensions where it is infrared- and ultraviolet-finite.

The box function analogous to L_{-1} , but for two adjacent external masses, is

$$\begin{aligned} L_{-1}^{2mh}(s, t; m_1^2, m_2^2) &= -\text{Li}_2\left(1 - \frac{m_1^2}{t}\right) - \text{Li}_2\left(1 - \frac{m_2^2}{t}\right) - \frac{1}{2} \ln^2\left(\frac{-s}{-t}\right) + \frac{1}{2} \ln\left(\frac{-s}{-m_1^2}\right) \ln\left(\frac{-s}{-m_2^2}\right) \\ &+ \left[\frac{1}{2}(s - m_1^2 - m_2^2) + \frac{m_1^2 m_2^2}{t} \right] I_3^{\text{m}}(s, m_1^2, m_2^2), \end{aligned} \quad (\text{I.3})$$

where I_3^{m} is the three-mass scalar triangle integral. Here we use only a version of this box function with I_3^{m} removed,

$$\widetilde{L}_{-1}^{2mh}(s, t; m_1^2, m_2^2) = -\text{Li}_2\left(1 - \frac{m_1^2}{t}\right) - \text{Li}_2\left(1 - \frac{m_2^2}{t}\right) - \frac{1}{2} \ln^2\left(\frac{-s}{-t}\right) + \frac{1}{2} \ln\left(\frac{-s}{-m_1^2}\right) \ln\left(\frac{-s}{-m_2^2}\right). \quad (\text{I.4})$$

The analytic properties of these integrals are straightforward to obtain from the prescription of adding a small positive imaginary part to each invariant, $s_{ij} \rightarrow s_{ij} + i\varepsilon$. One expands the logarithmic ratios, $\ln(r) \equiv \ln(\frac{-s}{-s'}) = \ln(-s) - \ln(-s')$, and then uses

$$\ln(-s - i\varepsilon) = \ln|s| - i\pi\Theta(s). \quad (\text{I.5})$$

where $\Theta(s)$ is the step function: $\Theta(s > 0) = 1$ and $\Theta(s < 0) = 0$. The imaginary part of the dilogarithm $\text{Li}_2(1-r)$ is given in terms of the logarithmic ratio,

$$\text{Im Li}_2(1-r) = -\ln(1-r) \text{Im ln}(r). \quad (\text{I.6})$$

For $r > 0$ the real part of $\text{Li}_2(1-r)$ is given directly by eq. (I.2). For $r < 0$ one may use [33]

$$\text{Re Li}_2(1-r) = \frac{\pi^2}{6} - \ln|r| \ln|1-r| - \text{Re Li}_2(r), \quad (\text{I.7})$$

with $\text{Re Li}_2(r)$ given by eq. (I.2).

The analytic structure of I_3^{3m} is more complicated [34,35,36], and the numerical representation we use depends on the kinematics. The integral is defined by

$$I_3^{\text{3m}}(s_{12}, s_{34}, s_{56}) = \int_0^1 d^3 a_i \delta(1 - a_1 - a_2 - a_3) \frac{1}{-s_{12}a_1a_2 - s_{34}a_2a_3 - s_{56}a_3a_1}. \quad (\text{I.8})$$

This integral is symmetric under any permutation of its three arguments, and acquires a minus sign when the signs of all three arguments are simultaneously reversed. Therefore we only have to consider two cases,

1. The Euclidean region $s_{12}, s_{34}, s_{56} < 0$, which is related by the sign flip to the pure Minkowski region ($s_{12}, s_{34}, s_{56} > 0$) relevant for e^+e^- annihilation. Here the imaginary part vanishes. This region has two subcases, depending on the sign of the Gram determinant $\Delta_3(s_{12}, s_{34}, s_{56})$ defined in eq. (3.6):

1a. $\Delta_3 < 0$,

1b. $\Delta_3 > 0$.

2. The mixed region $s_{12}, s_{56} < 0$, $s_{34} > 0$, for which Δ_3 is always positive.

In region 1a one may use a symmetric representation found by Lu and Perez [34], which is closely related to that given in ref. [36]:

$$I_3^{\text{3m}} = \frac{2}{\sqrt{-\Delta_3}} \left[\text{Cl}_2 \left(2 \tan^{-1} \left(\frac{\sqrt{-\Delta_3}}{\delta_{12}} \right) \right) + \text{Cl}_2 \left(2 \tan^{-1} \left(\frac{\sqrt{-\Delta_3}}{\delta_{34}} \right) \right) + \text{Cl}_2 \left(2 \tan^{-1} \left(\frac{\sqrt{-\Delta_3}}{\delta_{56}} \right) \right) \right], \quad (\text{I.9})$$

where the δ_{ij} are defined in eq. (3.6) and the Clausen function $\text{Cl}_2(x)$ is defined by

$$\text{Cl}_2(x) \equiv \sum_{n=1}^{\infty} \frac{\sin(nx)}{n^2} = - \int_0^x dt \ln(|2 \sin(t/2)|). \quad (\text{I.10})$$

In regions 1b and 2 a convenient representation is given by Ussyukina and Davydychev [35],

$$I_3^{\text{3m}} = -\frac{1}{\sqrt{\Delta_3}} \text{Re} \left[2 (\text{Li}_2(-\rho x) + \text{Li}_2(-\rho y)) + \ln(\rho x) \ln(\rho y) + \ln\left(\frac{y}{x}\right) \ln\left(\frac{1+\rho y}{1+\rho x}\right) + \frac{\pi^2}{3} \right] \\ - \frac{i\pi\Theta(s_{34})}{\sqrt{\Delta_3}} \ln \left(\frac{(\delta_{12} + \sqrt{\Delta_3})(\delta_{56} + \sqrt{\Delta_3})}{(\delta_{12} - \sqrt{\Delta_3})(\delta_{56} - \sqrt{\Delta_3})} \right), \quad (\text{I.11})$$

where

$$x = \frac{s_{12}}{s_{56}}, \quad y = \frac{s_{34}}{s_{56}}, \quad \rho = \frac{2s_{56}}{\delta_{56} + \sqrt{\Delta_3}}. \quad (\text{I.12})$$

Finally, in the top quark contribution to A_6^{ax} the combination $f(m_t) - f(m_b)$ appears, where $f(m)$ is the integral

$$f(m; s_{12}, s_{34}, s_{56}) = \int_0^1 d^3 a_i \delta(1 - a_1 - a_2 - a_3) \frac{a_2 a_3}{m^2 - s_{12}a_1a_2 - s_{34}a_2a_3 - s_{56}a_3a_1}. \quad (\text{I.13})$$

This integral is complicated for arbitrary mass m ; however, the large and small mass limits of it suffice for m_t and m_b respectively. For $m = m_t$ we simply Taylor expand the integrand in $1/m$; for $m = m_b$ we set m_b to zero, and reduce $f(0)$ to a linear combination of the massless scalar triangle integral I_3^{3m} given above, logarithms and rational functions. We get

$$\begin{aligned}
f(m_t; s_{12}, s_{34}, s_{56}) &= \frac{1}{24m_t^2} + \frac{(2s_{34} + s_{12} + s_{56})}{360m_t^4} + \dots, \\
f(0; s_{12}, s_{34}, s_{56}) &= \left(\frac{3s_{34}\delta_{34}}{\Delta_3^2} - \frac{1}{\Delta_3} \right) s_{12}s_{56}I_3^{\text{3m}}(s_{12}, s_{34}, s_{56}) + \left(\frac{3s_{56}\delta_{56}}{\Delta_3^2} - \frac{1}{2\Delta_3} \right) s_{12} \ln \left(\frac{-s_{12}}{-s_{34}} \right) \\
&\quad + \left(\frac{3s_{12}\delta_{12}}{\Delta_3^2} - \frac{1}{2\Delta_3} \right) s_{56} \ln \left(\frac{-s_{56}}{-s_{34}} \right) - \frac{\delta_{34}}{2\Delta_3}.
\end{aligned} \tag{I.14}$$

References

- [1] J. Ellis, M.K. Gaillard and G.G. Ross, Nucl. Phys. B111:253 (1976).
- [2] A. Ali, et al., Phys. Lett. 82B:285 (1979); Nucl. Phys. B167:454 (1980).
- [3] R.K. Ellis, D.A. Ross and A.E. Terrano, Phys. Rev. Lett. 45:1226 (1980); Nucl. Phys. B178:421 (1981);
K. Fabricius, I. Schmitt, G. Kramer and G. Schierholz, Phys. Lett. B97:431 (1980); Z. Phys. C11:315 (1981).
- [4] K. Hagiwara and D. Zeppenfeld, Nucl. Phys. B313:560 (1989);
F.A. Berends, W.T. Giele and H. Kuijf, Nucl. Phys. B321:39 (1989);
N.K. Falk, D. Graudenz and G. Kramer, Nucl. Phys. B328:317 (1989).
- [5] Z. Kunszt and P. Nason, in Z Physics at LEP1, CERN Yellow Report 89-08;
G. Kramer and B. Lampe, Z. Phys. C34:497 (1987); C42:504(E) (1989); Fortschr. Phys. 37:161 (1989);
W.T. Giele and E.W.N. Glover, Phys. Rev. D46:1980 (1992);
S. Catani and M.H. Seymour, Phys. Lett. B378:287 (1996), hep-ph/9602277.
- [6] OPAL Collab., P.D. Acton et al., Z. Phys. C55:1 (1992);
ALEPH Collab., D. Decamp et al., Phys. Lett. B284:163 (1992);
L3 Collab., O. Adriani et al., Phys. Lett. B284:471 (1992);
DELPHI Collab., P. Abreu et al., Z. Phys. C59:21 (1993);
SLD Collab., K. Abe et al., Phys. Rev. D51:962 (1995).
- [7] S. Dawson, E. Eichten and C. Quigg, Phys. Rev. D31:1581 (1985);
R.M. Barnett, H.E. Haber and G.L. Kane, Nucl. Phys. B267:625 (1986);
L. Clavelli, Phys. Rev. D46:2112 (1992);
J. Ellis, D. Nanopoulos, and D. Ross, Phys. Lett. B305:375 (1993), hep-ph/9303273;
L. Clavelli, P. Coulter and K. Yuan, Phys. Rev. D47:1973 (1993), hep-ph/9205237;
R. Muñoz-Tapia and W.J. Stirling, Phys. Rev. D49:3763 (1994), hep-ph/9309246;
G.R. Farrar, Phys. Rev. D51:3904 (1995), hep-ph/9407401; preprint hep-ph/9504295; preprint hep-ph/9508291; preprint hep-ph/9508292;
L. Clavelli, I. Terekhov, Phys. Rev. Lett. 77:1941 (1996), hep-ph/9605463; hep-ph/9603390;
A. de Gouvea and H. Murayama, preprint hep-ph/9606449;
Z. Bern, A.K. Grant, A.G. Morgan, preprint hep-ph/9606466.
- [8] Z. Bern, L. Dixon and D.A. Kosower, preprint hep-ph/9606378.
- [9] Z. Bern, L. Dixon and D.A. Kosower, in preparation.
- [10] A. Signer and L. Dixon, preprint hep-ph/9609460.

- [11] E.W.N. Glover and D.J. Miller, preprint hep-ph/9609474.
- [12] Z. Bern, L. Dixon and D.A. Kosower, to appear in *Annual Reviews of Nuclear and Particle Science* (1996), hep-ph/9602280.
- [13] Z. Bern, L. Dixon and D.A. Kosower, Phys. Rev. Lett. 70:2677 (1993), hep-ph/9302280.
- [14] Z. Kunszt, A. Signer and Z. Trócsányi, Phys. Lett. B336:529 (1994), hep-ph/9405386.
- [15] Z. Bern, L. Dixon and D.A. Kosower, Nucl. Phys. B437:259 (1995), hep-ph/9409393.
- [16] Z. Bern, G. Chalmers, L. Dixon and D.A. Kosower, Phys. Rev. Lett. 72:2134 (1994), hep-ph/9312333.
- [17] G.D. Mahlon, Phys. Rev. D49:2197 (1994), hep-ph/9311213; Phys. Rev. D49:4438 (1994), hep-ph/9312276.
- [18] Z. Bern, L. Dixon, D.C. Dunbar and D.A. Kosower, Nucl. Phys. B425:217 (1994), hep-ph/9405248.
- [19] Z. Bern, L. Dixon, D.C. Dunbar and D.A. Kosower, Nucl. Phys. B435:39 (1995), hep-ph/9409265.
- [20] L.D. Landau, Nucl. Phys. 13:181 (1959);
S. Mandelstam, Phys. Rev. 112:1344 (1958), 115:1741 (1959);
R.E. Cutkosky, J. Math. Phys. 1:429 (1960).
- [21] Z. Bern and A.G. Morgan, Nucl. Phys. B467:479 (1996), hep-ph/9511336.
- [22] Z. Bern and G. Chalmers, Nucl. Phys. B447:465 (1995), hep-ph/9503236.
- [23] F.A. Berends, R. Kleiss, P. De Causmaecker, R. Gastmans and T. T. Wu, Phys. Lett. 103B:124 (1981);
P. De Causmaecker, R. Gastmans, W. Troost and T.T. Wu, Nucl. Phys. B206:53 (1982);
R. Kleiss and W.J. Stirling, Nucl. Phys. B262:235 (1985);
R. Gastmans and T.T. Wu, *The Ubiquitous Photon: Helicity Method for QED and QCD* (Clarendon Press, 1990);
Z. Xu, D.-H. Zhang and L. Chang, Nucl. Phys. B291:392 (1987).
- [24] J.F. Gunion and Z. Kunszt, Phys. Lett. 161B:333 (1985).
- [25] F.A. Berends and W.T. Giele, Nucl. Phys. B294:700 (1987);
M. Mangano, S. Parke and Z. Xu, Nucl. Phys. B298:653 (1988);
Z. Bern and D.A. Kosower, Nucl. Phys. B362:389 (1991).
- [26] M. Mangano and S.J. Parke, Phys. Rep. 200:301 (1991);
L. Dixon, preprint hep-ph/9601359, to appear in *Proceedings of TASI 95*, ed. D.E. Soper.
- [27] J.C. Collins, *Renormalization* (Cambridge University Press, 1984).
- [28] Z. Bern and D.A. Kosower, Phys. Rev. Lett. 66:1669 (1991);
Z. Bern and D.A. Kosower, Nucl. Phys. B379:451 (1992).
- [29] Z. Kunszt, A. Signer and Z. Trócsányi, Nucl. Phys. B411:397 (1994), hep-ph/9305239;

- A. Signer, Ph.D. thesis, ETH Zürich (1995).
- [30] W. Siegel, Phys. Lett. 84B:193 (1979);
D.M. Capper, D.R.T. Jones and P. van Nieuwenhuizen, Nucl. Phys. B167:479 (1980);
L.V. Avdeev and A.A. Vladimirov, Nucl. Phys. B219:262 (1983).
 - [31] K. Hikasa, Mod. Phys. Lett. A5:1801 (1990);
K. Hagiwara, T. Kuruma and Y. Yamada, Nucl. Phys. B358:80 (1991).
 - [32] Z. Bern, hep-ph/9304249, in *Proceedings of Theoretical Advanced Study Institute in High Energy Physics (TASI 92)*, eds. J. Harvey and J. Polchinski (World Scientific, 1993);
Z. Bern and A.G. Morgan, Phys. Rev. D49:6155 (1994), hep-ph/9312218;
A.G. Morgan, Phys. Lett. B351:249 (1995), hep-ph 9502230.
 - [33] L. Lewin, *Dilogarithms and Associated Functions* (Macdonald, 1958).
 - [34] H.-J. Lu and C. Perez, preprint SLAC-PUB-5809 (1992).
 - [35] N.I. Ussyukina and A.I. Davydychev, Phys. Lett. 298B:363 (1993).
 - [36] Z. Bern, L. Dixon and D.A. Kosower, Nucl. Phys. B412:751 (1994), hep-ph/9306240.